Dalton Transactions

RSC Publishing

PAPER

View Article Online
View Journal

Cite this: DOI: 10.1039/c2dt32695g

Sequential ROMP of cyclooctenes as a route to linear polyethylene block copolymers†

Louis M. Pitet, Jihua Zhang and Marc A. Hillmyer*

Received 12th November 2012,
Accepted 18th December 2012

DOI: 10.1039/c2dt32695g

www.rsc.org/dalton

AB diblock copolymers were prepared by sequential ring-opening metathesis polymerization of cyclooctenes catalyzed by a Ru-based Grubbs catalyst. The relatively slow polymerization of *cis*-3-phenylcyclooct-1-ene (3PC) or *cis*-cyclooct-2-en-1-yl acetate (3AC) was first carried out and then followed by the faster polymerization of unsubstituted *cis*-cyclooctene (COE) from the active Ru-alkylidene chain ends. In contrast, simultaneous polymerization of the two monomers provides copolymers with a statistical monomer distribution owing to extensive chain transfer. The resulting poly(3PC-*b*-COE) and poly(3AC-*b*-COE) diblock copolymers were subjected to hydrogenation to selectively saturate the backbone alkenes. The consequences of architectural variance between the materials from simultaneous *vs.* sequential polymerizations are reflected by the contrasting thermal characteristics.

Introduction

Linear polyethylene (LPE) has long been the world's largest volume commodity polymer. LPE constitutes an indispensible part of daily life, being commonly used for everything from food storage to transportation to biomedical devices. LPE owes its versatility to its durability, ductility, toughness, corrosion resistance, and broad use temperature range (T_m = 130 °C; T_g < −100 °C). Enhancing the properties of LPE-based plastics by introducing functionality or increasing compositional complexity remains appealing, driven by the desire to address a broader range of applications.[1–5]

Block copolymers typically undergo microphase separation, adopting composition-dependent morphologies comprising domains with nanoscopic dimensions.[6] Block copolymers embody the physical attributes of each constituent combined with unique properties derived specifically from the microphase separation. Preparation of block copolymers that contain LPE typically requires elaborate synthetic protocols, which most often involve mechanistic transformations.[7] The last decade has witnessed tremendous progress in functional group tolerance during coordination and metallocene polymerization of vinyl monomers,[8–10] ultimately allowing precise functionalization of LPE (and copolymers) and transformation to alternate mechanisms (*e.g.*, ATRP[11–14] and ring-opening transesterification polymerization or ROTEP[15–17]) or coupling reactions to form block copolymers.[18–20]

As an alternative, organometallic mediated metathesis polymerization in concert with hydrogenation can yield completely linear polyethylene having a wide variety of functionality.[21,22] Chain transfer agents (CTAs) employed during ring-opening metathesis polymerization (ROMP) of cyclic olefins have been used to prepare telechelic polyolefins with functional groups capable of subsequent transformation to RAFT polymerization,[23] ATRP,[24,25] NMP,[26] anionic polymerization[27,28] and ROTEP,[29–31] collectively generating a rich variety of block copolymers with many potential uses.[32] From a practical perspective, however, it is more appealing to prepare such copolymers in a single-pot, making use of a single polymerization mechanism.

Indeed, block copolymers with LPE have been prepared by sequential living ROMP using Mo-based catalysts and employing cyclopentene monomer to generate the LPE segments (after hydrogenation).[33–36] Ru-based catalysts recently described by Vougioukalakis and Grubbs[37] have emerged as indispensible tools for making complex, functional, multicomponent block copolymers. The controlled nature of polymerizations using certain catalyst derivatives allows multiple monomers to be sequentially polymerized to form discrete, chemically distinct blocks.[38,39] The isodesmic nature of the ROMP reactions leaves double bonds in the backbone that are prone to secondary metathesis in a chain transfer process. Extensive chain transfer leads to randomization (*i.e.*, redistribution) of the monomer sequence. The extent to which the repeating unit sequences are redistributed depends largely on the steric environment around the double bond after ring-opening; less sterically encumbered backbones will undergo more secondary metathesis. Therefore, living polymerizations and block copolymers are most typically formed using bulky monomers like

Department of Chemistry, University of Minnesota, Twin Cities, 207 Pleasant Street SE, Minneapolis, Minnesota 55455-0431, USA. E-mail: hillmyer@umn.edu

†Electronic supplementary information (ESI) available: Experimental details, spectra, and thermographs. See DOI: 10.1039/c2dt32695g

substituted norbornenes.[40,41] Creating block copolymers by ROMP that contain poly(cyclooctene) (PCOE), a common precursor to LPE, has been challenging.[42]

One strategy that has been employed to form block copolymers involves first a bulky monomer followed by a less encumbered one. The sequence of polymerization must be in that particular order such that the second monomer polymerizes very quickly and any cross-metathesis during polymerization will be with the second block as opposed to the first bulky repeating unit.[43] For example, cyclooctene and cyclooctadiene are both consumed very quickly but undergo substantial cross metathesis during polymerization using conventional ruthenium catalysts, and therefore give polymers with relatively broad molar mass distribution.[44,45] This sequential polymerization strategy has been employed with the bulky carbazole-substituted norbornene, for example.[43,46] Likewise, sequential polymerization of *exo-N*-arylnorbornene-2,3-dicarboximides followed by dioxepine led to blocky polymer architectures.[47–49] Additionally, Coughlin and coworkers employed different solvents to adjust the relative polymerization rates between COE and functionalized norbornenes. In this way, either short (nearly alternating) sequences or long sequences of each monomer were accessible, despite the simultaneous, single pot reaction conditions.[50] In this work we describe a new synthetic approach to block copolymers that contain LPE by sequential polymerization of cyclooctenes.

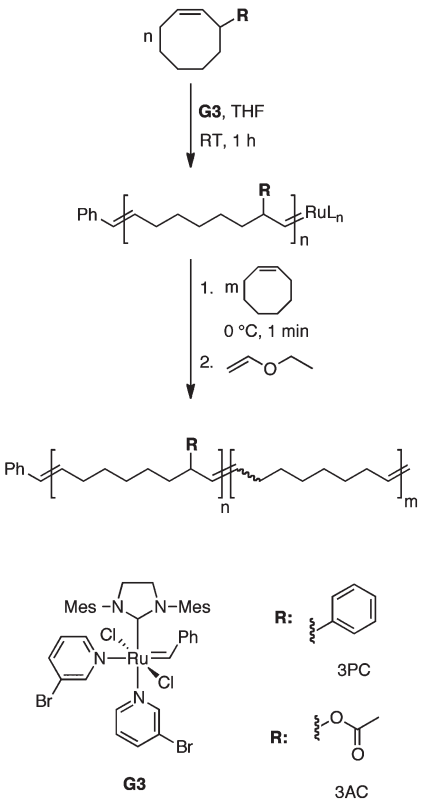

Scheme 1 Sequential polymerization of 3PC or 3AC and COE monomers to form poly(3PC-*b*-COE) or poly(3AC-*b*-COE) diblock copolymers.

Results and discussion

The synthesis of block copolymers from sequential polymerization of two monomers by ROMP was achieved by using the 3-bromopyridine ligated derivative of the ruthenium-based Grubbs catalyst (**G3**) (Scheme 1).[51] The catalyst **G3** gives high initiation and propagation rates during metathesis, and as such is conducive to living polymerizations of certain strained and sterically bulky cyclic olefins.[51,52] Either *cis*-3-phenylcyclooct-1-ene (3PC) or *cis*-cyclooct-2-en-1-yl acetate (3AC) was polymerized first.[53,54] After nearly complete monomer consumption, the second monomer *cis*-cyclooctene (COE) was added and rapidly consumed. The reaction was quenched with ethyl vinyl ether, and the polymer isolated by precipitation. The unsaturated diblock copolymers poly(3PC-*b*-COE) and poly(3AC-*b*-COE) were saturated by chemical hydrogenation with *p*-tosyl hydrazide to form a diblock copolymer containing a phenyl- or acetoxy-substituted polyethylene block and a completely linear polyethylene block, *h*-poly(3PC-*b*-COE) or *h*-poly(3AC-*b*-COE), respectively.

The 3PC monomer was prepared by brominating COE in the allyl position followed by CuI catalyzed Grignard substitution using phenyl magnesium bromide (Scheme S1, ESI†).[55] 3AcCOE was synthesized by hydrolyzing the brominated COE followed by acetylation of the resulting 3-hydroxy COE (Scheme S1†).[54] The first monomer was polymerized in THF at ambient temperature after initiation with **G3**. An aliquot was removed and analyzed by ^{1}H and ^{13}C nuclear magnetic resonance (NMR) spectroscopy after precipitation in cold MeOH (Fig. S1†). Polymerization of 3PC and 3AC catalyzed by **G3** proceeds in a regio- and stereo-specific manner as confirmed by NMR spectroscopy (see ESI Fig. S2†).[53] At RT the polymerization of 3PC/3AC progresses slowly relative to the unsubstituted COE analog using **G3**.[56]

Intramolecular cross metathesis during polymerization manifests itself in the (re)distribution of chain end functionalization. Therefore a small proportion of chains will be nonfunctional, having benzylidene groups at both chain termini and an equal proportion of chains will contain active Ru at both chain termini. Upon subsequent monomer addition, this scenario will result in a mixture of homopolymer poly(3PC) (or poly(3AC)), diblock copolymer, and symmetric triblock copolymer assuming the absence of interblock chain transfer in the second polymerization step.

Chain extension was performed to synthesize block copolymers from the polymerization solution containing poly(3PC) (or poly(3AC)) with metathesis-active Ru-alkylidene chain ends (Scheme 1). After one hour of 3PC (or 3AC) homopolymerization, the solution was cooled to ~5 °C using an ice bath and unsubstituted COE was added to the polymerization solution under an argon atmosphere. The polymerization solution became extremely viscous within 5 seconds, consistent with fast polymerization of COE using **G3** compared to 3PC (or 3AC). Prior to termination, chain transfer with the poly(3PC) (or poly(3AC)) block during COE polymerization is minimal

Table 1 Molecular and composition targets and experimental values for poly(3PC-*b*-COE) and poly(3AC-*b*-COE) block copolymers and the precursors[a]

Sample	N_{target}	M_n, target (kg mol^{-1})	Target		Experimental	
			w_{COE}[b]	n_{COE}[c]	w_{COE}[b]	n_{COE}[c]
poly(3PC)-170	170	31.6				
poly(3PC$_{25}$-*b*-COE$_{75}$)	950	117	0.73	0.82	0.76	0.84
poly(3PC)-950	950	177				
poly(3PC$_{40}$-*b*-COE$_{60}$)	1600	353	0.50	0.63	0.62	0.73
poly(3PC)-100	100	18.6				
poly(3PC$_{50}$-*b*-COE$_{50}$)	250	35.1	0.50	0.63	0.52	0.65
poly(3AC)-100	100	16.8				
poly(3AC$_{25}$-*b*-COE$_{75}$)	550	66.4	0.75	0.82	0.74	0.81
poly(3AC)-200	200	33.6				
poly(3AC$_{50}$-*b*-COE$_{50}$)	500	66.7	0.50	0.60	0.45	0.56
poly(3AC)-300	300	50.5				
poly(3AC$_{75}$-*b*-COE$_{25}$)	450	67.0	0.25	0.34	0.16	0.23

[a] The samples are labeled in accordance with the approximate measured compositions by ^{1}H NMR spectroscopy; the labels are poly(3PC$_x$-*b*-COE$_y$) or poly(3AC$_x$-*b*-COE$_y$), where x and y are the wt% of the respective blocks (*i.e.*, $x + y = 100$). [b] w_{COE} is the weight fraction of cyclooctene monomer. [c] n_{COE} is the mole fraction of cyclooctene.

such that polymer structure contains predominantly a diblock architecture. Intrablock chain transfer within the PCOE block as COE polymerization proceeds has been established for the Grubbs ruthenium-benzylidene catalyst systems having N-heterocyclic carbene ligands and presumably occurs in this chain extension process, leading to a broadened molar mass distribution ($Đ \rightarrow 2$). Nevertheless, the architecture should be blocky with the number-average molar mass dictated by the initial **G3** concentration.

Several samples were prepared by the method described. The targeted degrees of polymerization for a series of homopolymer precursors and the corresponding diblock copolymers are shown in Table 1 along with the experimentally determined values for composition by ^{1}H NMR spectroscopy (Fig. S3 and S4†).

As an example, analysis of the first poly(3PC)-170 and the resulting copolymer poly(3PC$_{25}$-*b*-COE$_{75}$) block by size-exclusion chromatography (SEC) after chain extension indicates an increase in molar mass (Fig. 1, *top*). The SEC chromatograms for poly(3AC)-100 and the corresponding block copolymer poly(3AC$_{25}$-*b*-COE$_{75}$) are also indicative of substantive increase in molar mass after chain extension (Fig. 1, *bottom*). Collectively these suggest that the active catalyst remains on the chain ends of the first block, and that reinitiation occurs with high fidelity after the second monomer is added. The relative elution volumes are consistent with the targeted degrees of polymerization (see Table 1).[57] The larger breadth of the peak attributed to the block copolymer poly(3PC$_{25}$-*b*-COE$_{75}$) compared with the homopolymer poly(3PC)-170 suggests a larger molar mass distribution, which may be a consequence of substantial chain transfer during chain extension or homopolymer contamination from non-functional poly(3PC) (see ESI†).

The block copolymers containing 3PC monomer each had slightly higher PCOE content than originally targeted with the monomer feed compositions assuming quantitative monomer consumption. The diluted poly(3PC) block suggests

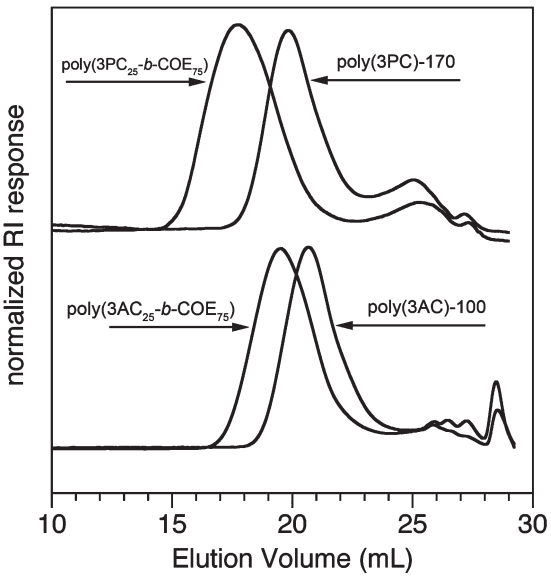

Fig. 1 Comparison of SEC chromatograms for (*top*) homopolymer poly(3PC)-170 and the block copolymer poly(3PC$_{25}$-*b*-COE$_{75}$) and (*bottom*) homopolymer poly(3AC)-100 and the block copolymer poly(3AC$_{25}$-*b*-COE$_{75}$).

incomplete consumption; the degree of conversion of 3PC for the sample poly(3PC$_{40}$-*b*-COE$_{60}$) was lower than in the sample poly(3PC$_{25}$-*b*-COE$_{75}$). Nonetheless, adjusting the monomer feed ratios allows control over the polymer composition.

It is the same scenario in the case of 3AC, for which the presence of acetoxy group at the allylic position reduces both the polymerization rate and the secondary metathesis rate relative to the unsubstituted COE. Three poly(3AC-*b*-COE) diblock copolymers that have similar molar mass but different weight fractions of the two blocks were synthesized in the same manner as for poly(3PC-*b*-COE) (Table 1). In all cases, ^{1}H NMR analysis was consistent with nearly complete consumption of monomer in both stages of the

polymerization, and all diblock copolymers exhibit a single and unimodal predominate peak in SEC.

We synthesized three additional copolymers by simultaneous polymerization of either 3PC or 3AC with COE, in an attempt to understand how critical the sequential polymerization protocol is for clean formation of block copolymer. Similar compositions as contained in the block copolymers (*i.e.*, those prepared *via* sequential monomer addition) were targeted. Two samples using 3PC were prepared by adding 1,4-diacetoxy-2-butene (DAB) with a given molar ratio to target N_{total} = ([3PC] + [COE])/[DAB] = 500.[58] A third sample using 3AC monomer was also prepared, with targeted degree of polymerization equal to 400. Table 2 contains the targeted and experimental molecular characteristics as measured by ^{1}H NMR spectroscopy (Fig. S5†). The SEC chromatograms for the statistical copolymers are all unimodal and nearly identical with respect to molar mass distribution and elution volume, suggesting effective chain transfer and molar mass control with the CTA addition (Fig. S6†).

Table 2 Molecular characteristics of statistical copolymers poly(3PC-*s*-COE) and poly(3AC-*s*-COE)

	Target			Experimental		
Sample	N^a	w_{PCOE}	n_{PCOE}	N^b	w_{PCOE}	n_{PCOE}
poly(3PC$_{25}$-*s*-COE$_{75}$)	500	0.75	0.84	484	0.76	0.84
poly(3PC$_{40}$-*s*-COE$_{60}$)	500	0.60	0.72	491	0.59	0.71
poly(3AC$_{60}$-*s*-COE$_{40}$)	400	0.40	0.50	420	0.39	0.48

[a] Calculated assuming quantitative monomer consumption, and taking the respective repeating units associated with the monomers. [b] Measured by ^{1}H NMR spectroscopy by comparing the integral ratios between the end groups and repeating units.

^{13}C NMR spectroscopy provides compelling evidence that the monomer sequence depends on the polymerization protocol (Fig. 2). The top two spectra in Fig. 2 (part a and d) show the respective homopolymers of poly(3PC) and poly(3AC), indicating a high degree of regio- and stereoregularity during ROMP with ruthenium-based catalysts. Only two olefinic signals are observed for both polymers, consistent with the previously reported structural assessment.[53] The block copolymers exhibit identical signals to the homopolymers along with two additional signals which are attributed to the *cis* and *trans* olefinic carbons from the PCOE blocks. These spectra suggest

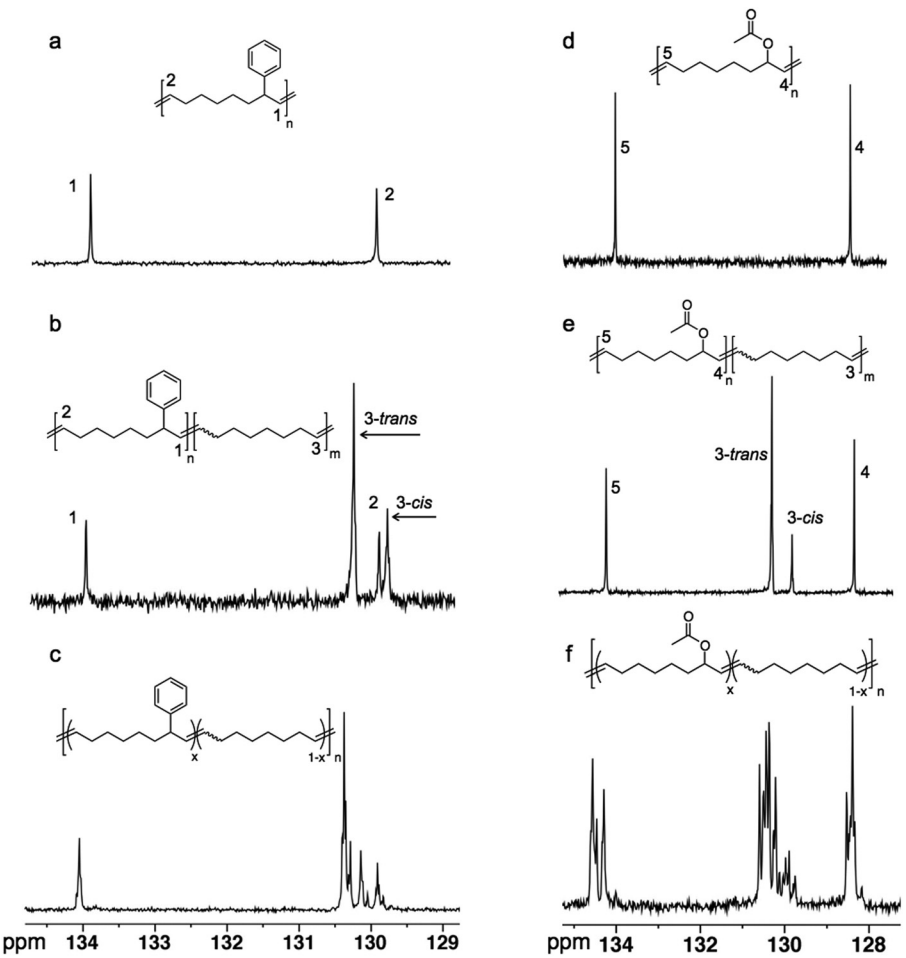

Fig. 2 Olefinic (and aromatic) region of ^{13}C NMR spectra for polymers (a) poly(3PC)-170; (b) poly(3PC$_{60}$-*b*-COE$_{40}$); (c) poly(3PC$_{60}$-*s*-COE$_{40}$); (d) poly(3AC)-100; (e) poly(3AC$_{50}$-*b*-COE$_{50}$) (f) poly(3AC$_{60}$-*s*-COE$_{40}$).

minimal contribution from a randomized repeating unit sequence distribution that would arise from extensive inter-block chain transfer. The spectra from two representative statistical copolymers show additional olefinic signals (Fig. 2c and 2e). This contrast can be attributed to various different segment lengths of repeating units with distinct electronic environments; this is a direct consequence of the polymerization protocol.

Thermal characteristics can also provide an indication of molecular architecture in copolymers. PCOE is a semi-crystalline polymer with a melting temperature near 50 °C.[59] The sequence length influences the capacity to organize into a crystalline lattice. The block and statistical architectures have contrasting thermal characteristics by differential scanning calorimetry (DSC) (Fig. 3).

The homopolymer PCOE (M_n = 50 kg mol^{-1}; $Đ$ = 1.8) prepared by ROMP shows a melting transition with peak T_m of 58 °C and a melting enthalpy (ΔH_m) of 69 J g^{-1}, corresponding to a calculated crystallinity of 32% (ΔH_m^0 = 216 J g^{-1}).[60] A weak glass transition was observed for the PCOE homopolymer near −80 °C. As a result of the bulky aryl substituents, homopolymer poly(3PC) is a sticky, liquid-like amorphous polymer with a low T_g (−20 °C; Fig. 3a). The block copolymer poly(3PC$_{25}$-*b*-COE$_{75}$) likewise shows a strong melting endotherm with T_m = 51 °C and a weak T_g at −69 °C. The slightly depressed T_m compared with PCOE is typical of block copolymers that undergo microphase separation in the melt. Likewise, the proximity of T_g to pristine PCOE suggests a microphase separated structure. The crystallinity of the poly(3PC$_{25}$-*b*-COE$_{75}$) is calculated as 27% (ΔH_m = 43.4 J g^{-1}; w_{PCOE} = 0.76), commensurate with a block architecture possessing only slightly less crystallinity within the majority PCOE matrix compared with the corresponding homopolymer. Similarly, poly(3PC$_{40}$-*b*-COE$_{60}$) shows a melting endotherm centered at 35 °C. While this value is lower than PCOE, the crystallinity is indicative of significantly long segments of PCOE in a blocky structure. The melting endotherm had an enthalpy ΔH_m of 16.1 J g^{-1}, corresponding to a crystallinity within the PCOE block of 12.4%.

The statistical copolymers show contrasting thermal behavior despite the nearly identical compositions (Fig. 3). The statistical copolymer poly(3PC$_{25}$-*s*-COE$_{75}$) exhibits a relatively weak melting endotherm with T_m = 22 °C and ΔH_m = 19.9 J g^{-1} corresponding to 12.3% crystallinity. Moreover, the poly(3PC$_{40}$-*s*-COE$_{60}$) has a pronounced T_g that is substantially depressed compared with homopolymer poly(3PC).

Similar thermal behavior was found apparent in poly(3AC-*b*-COE) (Fig. 3b). Homopolymer poly(3AC) is amorphous, exhibiting a T_g at −33 °C.[54] A nearly equivalent glass transition occurs for each of the poly(3AC-*b*-COE)s. Additionally, melting endotherms associated with the PCOE block were observed for all three samples. The melting temperature decreases with increasing content of poly(3AC) from 54 °C for poly(3AC$_{25}$-*b*-COE$_{75}$) to 51 °C for poly(3AC$_{50}$-*b*-COE$_{50}$) and to 43 °C

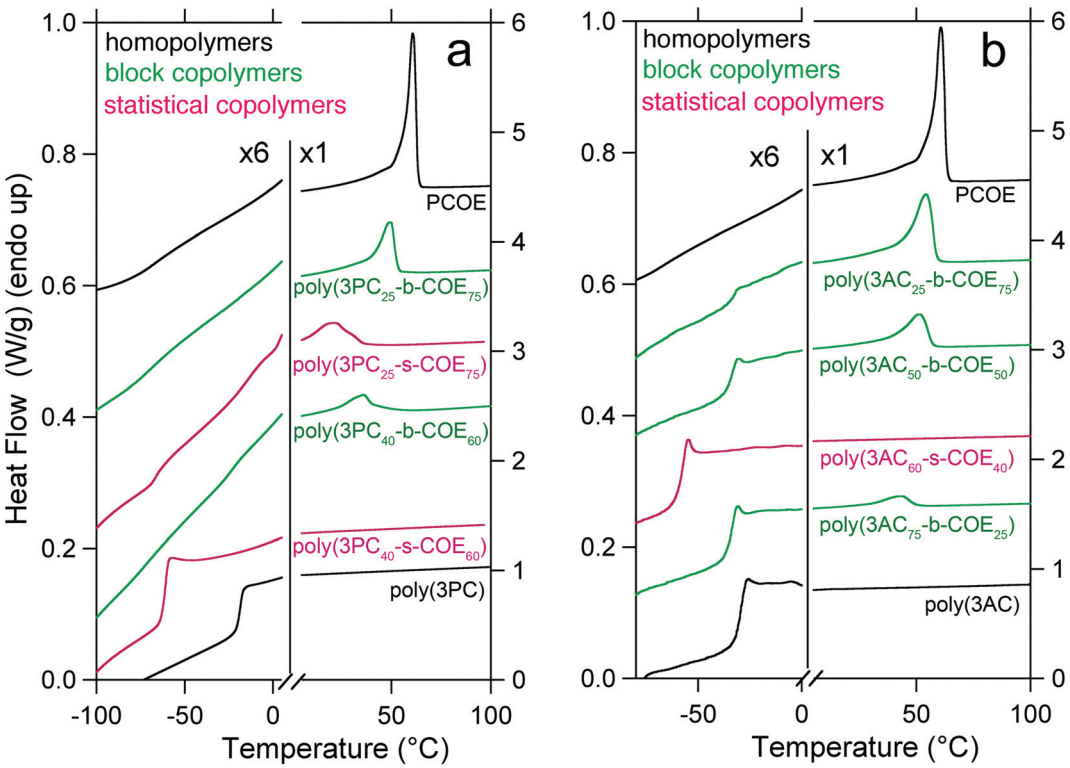

Fig. 3 DSC thermograms for (a) polycyclooctene (PCOE) homopolymer, block copolymers poly(3PC-*b*-COE)s, statistical copolymers poly(3PC-*s*-COE)s and poly(3PC) homopolymer and (b) PCOE homopolymer, block copolymers poly(3AC-*b*-COE)s, statistical copolymers poly(3AC-*s*-COE)s and poly(3AC) homopolymer. Individual thermograms have been shifted vertically for clarity. The left and right axes are at different scales to accentuate the low temperature glass transitions.

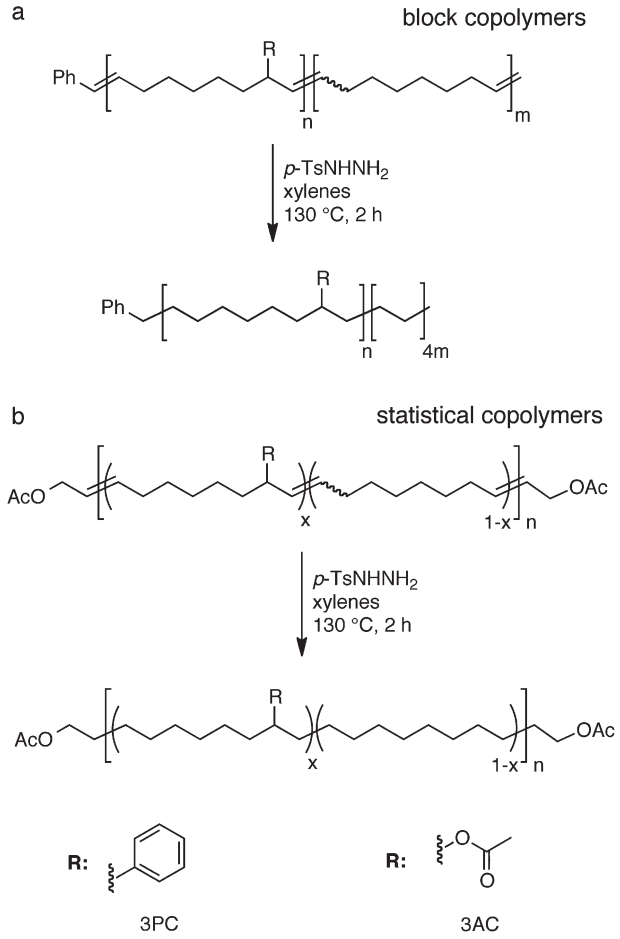

Scheme 2 Chemical hydrogenation of unsaturated block and statistical copolymers to form linear polyethylene copolymers (a) *h*-poly(3PC-*b*-COE) or *h*-poly(3AC-*b*-COE) and (b) *h*-poly(3PC-*s*-COE) or *h*-poly(3AC-*s*-COE).

for poly($3AC_{75}$-*b*-COE_{25}). Meanwhile, the melting enthalpy also decreases significantly, from 55.8 J g^{-1} to 30.5 J g^{-1} and to 10.4 J g^{-1}, which corresponds to a decrease of crystallinity within the PCOE block from 35% to 31% and to 30%, respectively. This behavior is consistent with microphase separation between the poly(3AC) and the PCOE domains in the poly(3AC-*b*-COE) samples. Comparatively, the statistical copolymer poly($3AC_{60}$-*s*-COE_{40}) displays a single T_g at −61 °C (Fig. 3b), which is intermediate between the two respective homopolymers suggesting a homogeneous microstructure.

The backbone double bonds in the copolymers were all saturated using *p*-tosyl hydrazide (*p*-$TsNHNH_2$) in xylenes at 130 °C (Scheme 2). Saturation extent of the copolymers was determined by ^1H NMR spectroscopy. The backbone alkene bonds are selectively hydrogenated to give LPE segments having sequential –CH_2– repeating units that have essentially equivalent chemical shifts at 1.3 ppm (Fig. S7†).[61] Importantly, the aryl substituents remain unsaturated as evidenced by the aromatic proton signals at a chemical shift of 7.3–7.1 ppm. The ratio of integrated signals associated with the aryl substituents and linear methylene repeat units agree within 5% of the original composition. The NMR spectra of all the block copolymers required high temperatures (100 °C in 1,1,2,2-tetrachloroethane), owing to the prohibitive solubility of LPE in all conventional solvents at ambient temperature. However the statistical copolymers *h*-poly(3AC-*s*-COE) were soluble in $CHCl_3$ at room temperature, a testament to the influence of polymerization protocol on sequence distribution and thus physical properties.

A sample of pristine PCOE (M_n = 50 kg mol^{-1}; $Đ$ = 1.8) was hydrogenated to generate LPE homopolymer for comparison with the block and statistical copolymers. Several samples of LPE (*h*-PCOE) show melting endotherms with relatively consistent T_m = 130–134 °C and ΔH_m = 165–200 J g^{-1} which corresponds to crystallinities in the vicinity of 60–72% (ΔH_m^0 = 277 J g^{-1}) (Fig. 4).[62] Homopolymer poly(3PC) and poly(3AC) were also hydrogenated to give *h*-poly(3PC) and *h*-poly(3AC) using an identical protocol (see ESI Fig. S7†). Samples of *h*-poly(3PC) are amorphous with T_g = −21 °C (Fig. 4a). The saturated block polymer *h*-poly($3PC_{25}$-*b*-COE_{75}) exhibits a similar melting endotherm to pristine LPE with a slightly depressed T_m of 120.5 °C, consistent with the decrease in melting temperature associated with block copolymers in which a semi-crystalline block is tethered to an amorphous block. The melting enthalpy ΔH_m = 101 J g^{-1} corresponds to 49% crystallinity within the LPE matrix component. A weak T_g can be observed near −20 °C (Fig. 4a). Likewise, the hydrogenated derivative *h*-poly($3PC_{40}$-*b*-COE_{60}) exhibits a glass transition at T_g = −18 °C, suggesting a block structure that undergoes microphase separation. The sample *h*-poly($3PC_{40}$-*b*-COE_{60}) also exhibits a melting endotherm at T_m = +115 °C and the melting enthalpy ΔH_m = 53 J g^{-1} corresponds to a crystallinity of approximately 32%.

The hydrogenated homopolymer of 3AC *h*-poly(3AC) is semi-crystalline with a T_m near 53 °C and a $T_g \approx -36$ °C.[54] These thermal features are found to be retained in the hydrogenated diblock copolymers *h*-poly(3AC-*b*-COE). In all three samples, there is a weak T_g in the range −30 to −35 °C and a T_m in the range 52 to 58 °C, while a second and more intense melting endotherm appears in the range 125 to 130 °C (Fig. 4b). The higher temperature T_m is attributed to the semi-crystalline LPE block and is slightly depressed compared with the T_m of pristine LPE. As the LPE content decreases in the diblock copolymer, the normalized melting enthalpy associated with the second melting peak drops from 185 to 138 J g^{-1} corresponding to a concomitant decrease in crystallinity from 67% to 50%. Distinct thermal behavior was observed with the saturated derivatives of the statistical copolymer (*h*-poly($3AC_{60}$-*s*-COE_{40})); it exhibits a broad endothermic transition with maximum close to 50 °C (Fig. 4b).

One dimensional X-ray scattering profiles taken at both small and large scattering angles were generated for LPE homopolymer sample[63] at ambient temperature after cooling from 160 °C (Fig. S9†). The small angle X-ray scattering (SAXS) plot shows the scattering intensity as a function of the spatial scattering vector $q = 4\pi(\sin\theta)\lambda^{-1}$, where 2θ is the scattering angle and λ is the wavelength of incident radiation (1.3776 Å).

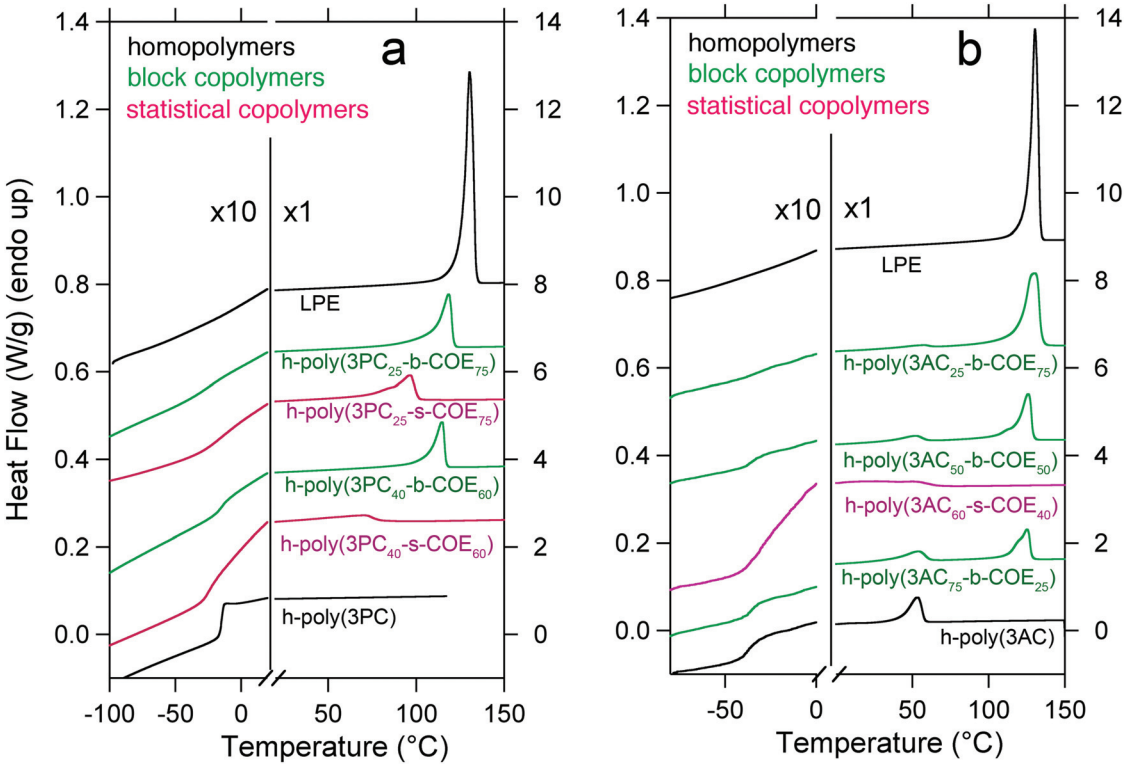

Fig. 4 DSC thermograms for (a) linear polyethylene (LPE) homopolymer, hydrogenated block copolymers *h*-poly(3PC-*b*-COE)s, statistical copolymers poly(3PC-*s*-COE)s and hydrogenated *h*-poly(3PC) homopolymer and (b) LPE homopolymer, hydrogenated block copolymers *h*-poly(3AC-*b*-COE)s and hydrogenated statistical copolymers *h*-poly(3AC-*s*-COE)s. Individual thermograms have been shifted vertically for clarity. The left and right axes are at different scales to accentuate the low temperature glass transitions.

The LPE sample shows two broad reflections located at approximately q = 0.28 and 0.60 nm^{-1}, respectively corresponding to dimensions (d) equal to 22 and 10 nm according to $d = 2\pi/q$. These reflections presumably arise from the periodic arrangement of alternating crystalline and amorphous lamellae ($q_2 : q_1 \approx 2 : 1$).

The wide-angle X-ray scattering (WAXS) profile contains two sharp peaks corresponding to the (110) and (200) planes at q = 15.4 and 17.1 nm^{-1}, respectively, associated with the orthorhombic crystal lattice conventionally adopted by LPE chains.[64] One-dimensional WAXS profiles for *h*-poly(3PC-*b*-COE) and *h*-poly(3AC-*b*-COE) reveal Bragg scattering reflections that are consistent with a substantial degree of crystallinity with identical orthorhombic lattice packing (Fig. 5a and 5b). This suggests considerably long segment lengths of LPE resulting from the block copolymerization–hydrogenation protocol, and the reversibility of the crystallization/melting process is illustrated with profiles after heating above T_m and subsequent cooling back to ambient temperature.

The WAXS measurement of the *h*-poly(3AC-*b*-COE) series shows the same LPE orthorhombic lattice scattering peaks and a small scattering signal at q = 10.1 nm^{-1} (Fig. 5b). The latter signal appears at the identical position as one of the scattering peaks seen for *h*-poly(3AC).[54] In the WAXS profile of *h*-poly-(3AC$_{75}$-*b*-COE$_{25}$) which has fairly high content of poly(3AC), the predominate signal splits into two peaks, a feature also observed for *h*-poly(3AC). This result suggests that both the LPE block and the saturated poly(3AC) block maintain crystal structures found in the corresponding homopolymers, an indication of efficient microphase separation. Furthermore, the scattering intensity of the LPE peaks decreases substantially with decreasing LPE content, which is in accordance with the decreased crystallinity within the LPE block indicated by the DSC result.

SAXS profiles for the block copolymer poly(3PC$_{50}$-*b*-COE$_{50}$) below the T_m reveal a distinct yet broad reflection centered at approximately q = 0.29 nm^{-1}, positioned nearly identically to the reflection seen in homopolymer LPE (Fig. 6a; Fig. S9†). It is evident that the polymer remains highly crystalline below 100 °C from simultaneously collected WAXS profiles (Fig. 6b).

However, above T_m the broad reflection in the SAXS profiles disappears, and is replaced by a relatively sharp reflection centered at q = 0.12 nm^{-1}. The sharp peak is consistent with a microphase separated, albeit disorganized morphology. The peak position corresponds to an average interdomain spacing d = 52 nm (according to $d = 2\pi/q$). These results suggest that (1) the prescribed sequential synthetic protocol does indeed lead to block copolymer architecture and (2) the sample is microphase separated at 150 °C.

The WAXS profiles for this sample are consistent with the DSC results, suggesting that the crystalline portions associated with LPE have melted at 150 °C, and that the crystallization/

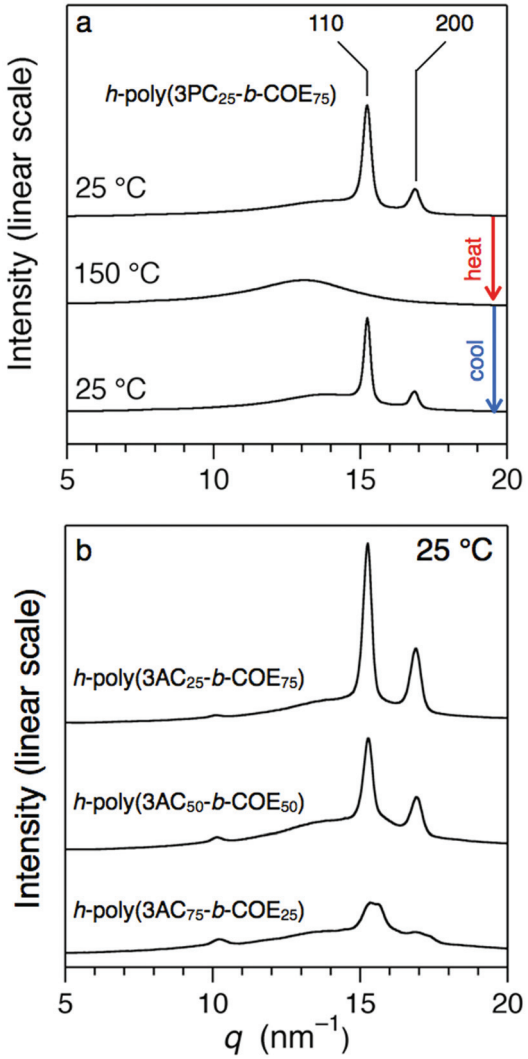

Fig. 5 One-dimensional WAXS profiles for the block copolymers (a) *h*-poly(3PC$_{25}$-*b*-COE$_{75}$) beginning at 25 °C, after heating to 150 °C (>$T_{m,LPE}$), and again after cooling back to ambient temperature (rate > 50 °C min^{-1}) and (b) *h*-poly(3AC$_{25}$-*b*-COE$_{75}$), *h*-poly(3AC$_{50}$-*b*-COE$_{50}$), and *h*-poly(3AC$_{75}$-*b*-COE$_{25}$) at 25 °C. Individual profiles have been shifted vertically for clarity.

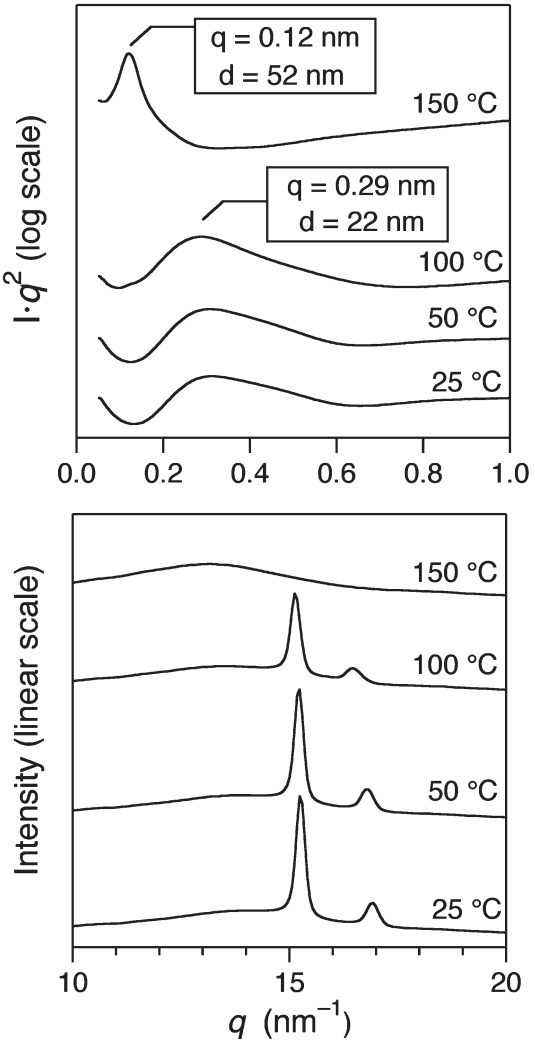

Fig. 6 One-dimensional scattering profiles for the block copolymer *h*-poly(3PC$_{50}$-*b*-COE$_{50}$) at (a) small angle and (b) wide angle beginning at 150 °C (>$T_{m,LPE}$) and cooling back to ambient temperature (rate > 50 °C min^{-1}). Profiles have been vertically shifted for clarity.

melting phenomena are reversible (Fig. 6b). These results corroborate the SAXS results, and the postulated relationship between crystal formation and microphase separation.

Conclusions

The synthetic strategy described here is a straightforward route to block copolymers with segments comprising high density polyethylene and aryl or acetoxy pendent groups. A diverse array of further possibilities can be imagined using this strategy. LPE imparts its superior qualities on hybrid materials with various functionalities by designing comonomers (*e.g.*, 3-substituted cyclooctenes). The relatively slow polymerization of *cis*-3-phenylcyclooct-1-ene was conducted followed by the fast polymerization of unsubstituted *cis*-cyclooctene to give copolymers having a blocky distribution of repeating units. In contrast, simultaneous polymerization of the two monomers provided copolymers with essentially statistical monomer distribution owing to extensive chain transfer. The architectural variance between the materials from simultaneous and sequential polymerizations was reflected by the thermal and molecular characteristics. The resulting poly(3-phenylcyclooctene-*block*-cyclooctene) diblock copolymers were subjected to hydrogenation to selectively saturate the backbone alkenes, leaving the pendent aryl substituents for further functionalization. Furthermore, the hydrogenated poly(3-acetoxycyclooctene-*block*-cyclooctene) diblock copolymers comprise two semi-crystalline blocks which display distinct melting temperatures and crystal structures. The saturated LPE backbone offers flexibility, strength, and resistance to chemical corrosion, and the potentially interesting consequences of

molecular architecture on mechanical performance is currently under investigation.

Acknowledgements

The authors acknowledge financial support from the National Science Foundation under contract DMR 1006370 as well as the Petroleum Institute of Abu Dhabi through the ADMIRE (Abu Dhabi-Minnesota Institute for Research Excellence) partnership. L.M.P. gratefully acknowledges support from the Doctoral Dissertation Fellowship awarded by the University of Minnesota Graduate School. We are indebted to Prof. Shingo Kobayashi for invaluable input. SAXS was performed at Beamline 5 (DND-CAT) at the Advanced Photon Source (APS). DND-CAT is supported by the Dow Chemical Company, E. I. DuPont de Nemours & Co., and the State of Illinois. Use of the APS was supported by the U.S. Department of Energy, Office of Science, Office of Basic Energy Sciences, under Contract No. DE-AC02-06CH11357.

Notes and references

1 S. B. Amin and T. J. Marks, *Angew. Chem., Int. Ed.*, 2008, **47**, 2006.
2 L. S. Boffa and B. M. Novak, *Chem. Rev.*, 2000, **100**, 1479.
3 N. C. Liu, W. E. Baker and K. E. Russell, *J. Appl. Polym. Sci.*, 1990, **41**, 2285.
4 I. A. I. Mkhalid, J. H. Barnard, T. B. Marder, J. M. Murphy and J. F. Hartwig, *Chem. Rev.*, 2009, **110**, 890.
5 G. Moad, *Prog. Polym. Sci.*, 1999, **24**, 81.
6 V. Abetz and P. F. W. Simon, *Adv. Polym. Sci.*, 2005, **189**, 125.
7 Y. Yagci and M. A. Tasdelen, *Prog. Polym. Sci.*, 2006, **31**, 1133.
8 E. Y. X. Chen, *Chem. Rev.*, 2009, **109**, 5157.
9 A. Nakamura, S. Ito and K. Nozaki, *Chem. Rev.*, 2009, **109**, 5215–5244.
10 M. Atiqullah, M. Tinkl, R. Pfaendner, M. N. Akhtar and I. Hussain, *Polym. Rev.*, 2010, **50**, 178.
11 H. Kaneyoshi, Y. Inoue and K. Matyjaszewski, *Macromolecules*, 2005, **38**, 5425.
12 H. Kaneyoshi and K. Matyjaszewski, *J. Appl. Polym. Sci.*, 2007, **105**, 3.
13 Y. Schneider, J. D. Azoulay, R. C. Coffin and G. C. Bazan, *J. Am. Chem. Soc.*, 2008, **130**, 10464.
14 Y. Schneider, N. A. Lynd, E. J. Kramer and G. C. Bazan, *Macromolecules*, 2009, **42**, 8763.
15 J. O. Ring, R. Thomann, R. Mulhaupt, J. M. Raquez, P. Degee and P. Dubois, *Macromol. Chem. Phys.*, 2007, **208**, 896.
16 C. J. Han, M. S. Lee, D.-J. Byun and S. Y. Kim, *Macromolecules*, 2002, **35**, 8923.
17 J. E. Baez, A. Ramirez-Hernandez and A. Marcos-Fernandez, *Polym. Adv. Technol.*, 2010, **21**, 55.
18 H. K. Kim, M. Zhang, X. Yuan, S. N. Lvov and T. C. M. Chung, *Macromolecules*, 2012, **45**, 2460.
19 T. Li, W. J. Wang, R. Liu, W. H. Liang, G. F. Zhao, Z. Li, Q. Wu and F. M. Zhu, *Macromolecules*, 2009, **42**, 3804.
20 Y. Zhao, L. Wang, A. Xiao and H. Yu, *Prog. Polym. Sci.*, 2010, **35**, 1195.
21 C. W. Bielawski and R. H. Grubbs, *Prog. Polym. Sci.*, 2007, **32**, 1.
22 T. W. Baughman and K. B. Wagener, *Adv. Polym. Sci.*, 2005, **176**, 1.
23 M. K. Mahanthappa, F. S. Bates and M. A. Hillmyer, *Macromolecules*, 2005, **38**, 7890.
24 C. W. Bielawski, T. Morita and R. H. Grubbs, *Macromolecules*, 2000, **33**, 678.
25 C. W. Bielawski, J. Louie and R. H. Grubbs, *J. Am. Chem. Soc.*, 2000, **122**, 12872.
26 S. M. Banik, B. L. Monnot, R. L. Weber and M. K. Mahanthappa, *Macromolecules*, 2011, **44**, 7141.
27 K. A. Switek, K. Chang, F. S. Bates and M. A. Hillmyer, *J. Polym. Sci., Part A: Polym. Chem.*, 2006, **45**, 361.
28 S. B. Myers and R. A. Register, *Macromolecules*, 2008, **41**, 5283.
29 L. M. Pitet, M. A. Amendt and M. A. Hillmyer, *J. Am. Chem. Soc.*, 2010, **132**, 8230.
30 L. M. Pitet, B. M. Chamberlain, A. W. Hauser and M. A. Hillmyer, *Macromolecules*, 2010, **43**, 8018.
31 L. M. Pitet and M. A. Hillmyer, *Macromolecules*, 2009, **42**, 3674.
32 S. Sutthasupa, M. Shiotsuki and F. Sanda, *Polym. J.*, 2010, **42**, 905.
33 S. Li, S. B. Myers and R. A. Register, *Macromolecules*, 2011, **44**, 8835.
34 S. B. Myers and R. A. Register, *Macromolecules*, 2008, **41**, 6773.
35 S. B. Myers and R. A. Register, *Macromolecules*, 2010, **43**, 393.
36 S. T. Trzaska, L.-B. W. Lee and R. A. Register, *Macromolecules*, 2000, **33**, 9215.
37 G. C. Vougioukalakis and R. H. Grubbs, *Chem. Rev.*, 2010, **110**, 1746.
38 S. Riegler, C. Slugovc, G. Trimmel and F. Stelzer, *Macromol. Symp.*, 2004, **217**, 231.
39 R. H. Grubbs and T. M. Trnka, *Ruthenium in Organic Synthesis*, 2004, p. 153.
40 K. Nomura and M. M. Abdellatif, *Polymer*, 2010, **51**, 1861.
41 A. Leitgeb, J. Wappel and C. Slugovc, *Polymer*, 2010, **51**, 2927.
42 R. Walker, R. M. Conrad and R. H. Grubbs, *Macromolecules*, 2009, **42**, 599.
43 J. Alonso-Villanueva, M. Rodriguez, J. L. Vilas, J. M. Laza and L. M. Leon, *J. Macromol. Sci., Part A: Pure Appl. Chem.*, 2010, **47**, 1130.
44 A. M. Alb, P. Enohnyaket, J. F. Craymer, T. Eren, E. B. Coughlin and W. F. Reed, *Macromolecules*, 2007, **40**, 444.

45 A. D. Benedicto, J. P. Claverie and R. H. Grubbs, *Macromolecules*, 1995, **28**, 500.
46 D. J. Liaw and P. L. Wu, *J. Mol. Catal. A: Chem.*, 2000, **160**, 35.
47 S. Hilf, E. Berger-Nicoletti, R. H. Grubbs and A. F. M. Kilbinger, *Angew. Chem., Int. Ed.*, 2006, **45**, 8045.
48 S. Hilf, R. H. Grubbs and A. F. M. Kilbinger, *Macromolecules*, 2008, **41**, 6006.
49 S. Hilf and A. F. M. Kilbinger, *Macromolecules*, 2009, **42**, 4127.
50 Y. C. Simon and E. B. Coughlin, *J. Polym. Sci., Part A: Polym. Chem.*, 2010, **48**, 2557.
51 J. A. Love, J. P. Morgan, T. M. Trnka and R. H. Grubbs, *Angew. Chem., Int. Ed.*, 2002, **41**, 4035.
52 T. M. Trnka, J. P. Morgan, M. S. Sanford, T. E. Wilhelm, M. Scholl, T. L. Choi, S. Ding, M. W. Day and R. H. Grubbs, *J. Am. Chem. Soc.*, 2003, **125**, 2546.
53 S. Kobayashi, L. M. Pitet and M. A. Hillmyer, *J. Am. Chem. Soc.*, 2011, **133**, 5794.
54 J. Zhang, M. E. Matta and M. A. Hillmyer, Manuscript in preparation.
55 N. Calderon, E. A. Ofstead and W. A. Judy, *J. Polym. Sci., Part A: Polym. Chem.*, 1967, **5**, 2209.
56 Preliminary kinetic experiments were conducted in deuterated THF in order to guage the approximate time required to reach maximum monomer conversion. Monomer/polymer concentrations were measured by NMR spectroscopy.
57 Homopolymerization of 3PC to form poly(3PC)-170 leads to a signal in the SEC chromatogram with a main peak centered at 20 mL elution volume and a less pronounced peak eluting later, centered near 25 mL, indicating a low molar mass portion. It is currently unclear from what process this stems.
58 The second generation derivative of Grubbs catalyst was used [Benzylidene[1,3-bis(2,4,6-trimethylphenyl)-2-imidazolidinylidene] dichloro (tricyclohexylphosphine) ruthenium, **G2**] because of its ready availability; the faster initiation rate touted with the **G3** is irrelevant when the CTA is being used for chain length control. The activity of **G2** and **G3** are comparable during polymerization due to the identical propagating residue after dissociation of the tricyclohexylphosphinyl or 3-bromopyridinyl ligands, respectively. The catalyst **G2** was added with the molar ratio ([3PC] + [COE])/[DAB]/[**G2**] = 10800/22/1.
59 N. Calderon and M. C. Morris, *J. Polym. Sci., Polym. Phys. Ed.*, 1967, **5**, 1283.
60 W. A. Schneider and M. F. Müller, *J. Mol. Catal.*, 1988, **46**, 395.
61 The saturation of the backbone of poly($3PC_{25}$-*b*-COE_{75}) was not quantitative as indicated by signals in the ^{1}H NMR spectrum associated with residual olefinic signals centered at a chemical shift of 5.5 ppm. The small olefinic residue remaining after hydrogenation of poly($3PC_{40}$-*b*-COE_{60}) may have occurred from the prohibitively large molar mass.
62 B. Wunderlich and M. Dole, *J. Polym. Sci.*, 1957, **24**, 201.
63 The linear polyethylene sample was synthesized by hydrogenating a PCOE sample with M_n = 50 kg mol^{-1} and $Đ$ = 1.8. The hydrogenation was performed with heterogeneous catalyst of 5% Pt/Re on silica in cyclohexane at 105 °C. Saturation was confirmed by ^{1}H NMR spectroscopy.
64 U. Gaur and B. Wunderlich, *J. Phys. Chem. Ref. Data*, 1981, **10**, 119.

